Microfluid Nanofluid (2015) 18:1195–1200
DOI 10.1007/s10404-014-1514-8

RESEARCH PAPER

Electrokinetically driven deterministic lateral displacement for particle separation in microfluidic devices

Srinivas Hanasoge · Raghavendra Devendra · Francisco J. Diez · German Drazer

Received: 12 June 2014 / Accepted: 3 November 2014 / Published online: 29 November 2014

Abstract An electrokinetically driven deterministic lateral displacement device is proposed for the continuous, two-dimensional fractionation of suspensions in microfluidic platforms. The suspended species are driven through an array of regularly spaced cylindrical posts by applying an electric field across the device. We explore the entire range of orientations of the driving field with respect to the array of obstacles and show that, at specific forcing angles, particles of different size migrate in different directions, thus enabling continuous, two-dimensional separation. We discuss a number of features observed in the motion of the particles, including directional locking and sharp transitions between migration angles upon variations in the direction of the force, that are advantageous for high-resolution two-dimensional separation. A simple model based on individual particle–obstacle interactions accurately describes the migration angle of the particles depending on the orientation of the driving field and can be used to reconfigure the electric field depending on the composition of the samples.

1 Introduction

A number of microfluidic devices have been proposed in recent years for the continuous separation of suspended particles employing novel techniques (Pamme 2007). A popular separation method is deterministic lateral displacement (DLD), in which a mixture of species is driven through an array of cylindrical posts. The interaction of the different species with the posts leads to different species migrating in different directions with respect to the array, thus causing the two-dimensional and continuous fractionation of the mixture (Huang et al. 2004; Inglis et al. 2006). Microfluidic DLD devices have been successfully applied to the fractionation of different mixtures, and in particular for cell sorting and the separation of biological material (Xuan and Lee 2013; Davis et al. 2006; Li et al. 2007; Huang et al. 2008; Morton et al. 2008a, b; Green et al. 2009; Holm et al. 2011; Inglis et al. 2011; Joensson et al. 2011; Zhang et al. 2012). In addition, different modifications of the original DLD design have been proposed for specific applications, such as the separation of deformable and nonspherical bioparticles (Al-Fandi et al. 2011; Zeming et al. 2013) or to improve performance (Loutherback et al. 2010; Beech and Tegenfeldt 2008; Beech et al. 2009). In recent work, we demonstrated a unique operating mode for high-purity DLD separation based on a uniform force driving the suspended particles, in particular gravity (g-DLD) (Devendra and Drazer 2012, 2014; Bowman et al. 2012). In terms of external fields, a variety of powerful separation methods take advantage of electric fields to drive the suspended mixture through a stationary phase to affect the separation, both in traditional and in microfluidic systems. In fact, arrays of insulating posts analogous to those found in DLD systems have been used in combination with DC electric fields for the continuous separation of particles by means of insulator-based dielectrophoresis (Cummings and Singh 2003; Cummings 2003). Moreover, the integration of insulator-based dielectrophoretic forces into DLD systems by adding AC electric fields has been shown to provide external control to the separation of different mixtures (Beech et al. 2009). Interestingly, virtual post arrays entirely based on negative DEP forces generated by patterned electrodes were successfully used to continuously separate particles by a method similar to DLD (Chang and

S. Hanasoge · R. Devendra · F. J. Diez · G. Drazer (✉)
Mechanical and Aerospace Engineering Department, Rutgers, The State University of New Jersey, Piscataway, NJ, USA
e-mail: german.drazer@rutgers.edu

Cho 2008). On the other hand, in spite of its potential, the use of electric fields to drive the suspended particles has not been investigated in DLD systems, possibly due to the fact that the original explanation of the separation phenomena observed in DLD systems was based on the flow field (Huang et al. 2004; Inglis et al. 2006). In previous work, however, we have shown in experiments and simulations that particle separation in DLD systems is induced by the cumulative and *separative* effect of particle–obstacle non-hydrodynamic interactions, whose presence is independent of the driving field (Balvin et al. 2009; Frechette and Drazer 2009; Herrmann et al. 2009; Bowman et al. 2013; Risbud and Drazer 2013).

Here, we demonstrate the simplicity and potential of electrokinetically driven DLD (e-DLD) separation devices using a simple microfluidic system that can be easily reconfigured to control the relative orientation of the driving field with respect to the array of posts. We performed detailed experiments tracking the motion of individual particles of three different sizes for the entire range of possible orientations of the driving electric field. We show that the motion of individual particles is completely analogous to that observed in flow- and force-driven DLD systems. More importantly, we identify specific angles at which different particles migrate in different directions within the array. Moreover, we show a significant difference in the migration angles, providing excellent size resolution and demonstrating the potential of e-DLD as a two-dimensional and continuous separation method. In addition to extending the versatility of DLD with an alternative driving field, the use of electric fields opens the possibility to online control of the orientation of the driving field depending on the sample.

2 Experimental

2.1 Materials and fabrication

The particles used in the experiments are: 4.32 μm (silica, density 2 g/cm^3, Bangs Laboratories, Inc., CA), 10 and 15 μm (glass, density 2.5 g/cm^3, Duke Scientific, CA). The particles were suspended in a 1 % aqueous solution of borate buffer to maintain a constant pH during the experiments. The array of cylindrical posts was fabricated in a negative photoresist (SU8 2025—Microchem Corp., MA) directly on a microscope glass slide using standard photolithography process. A picture of the device is shown in Fig. 1. The micro-posts were approximately 19 μm in diameter, 35 μm in height, and separated by 40 μm center-to-center. A channel fabricated in polydimethylsiloxane(PDMS) using softlitography methods was then used to cover the array of posts as indicated in Fig. 1. The dimensions of the channel were 50 μm in depth, 3 mm wide, and 2 cm long. Although the channel was higher than the obstacles, the particles settle to the bottom of the channel and move around the obstacles. Two relatively large reservoirs (1 cm × 0.5 cm, see Fig. 1) were punched into opposite ends of the PDMS channel to reduce the build-up of pressure during the experiments (Yan et al. 2006). A DC electric field of 60 V/cm (2400 Source Meter, Keithley) was applied using platinum electrodes introduced into the reservoirs.

2.2 Experimental setup and method

The applied electric field across the PDMS microchannel generates the electroosmotic flow that drives the particles. In addition, the particles experience an electrophoretic force that depends on their charge, but their motion is usually dominated by the electroosmotic flow, especially in buffered solutions (Hunter 1981; Masliyah and Bhattacharjee 2006; Paul et al. 1998; Sureda et al. 2012). The net velocity of the particles measured by tracking their trajectories was in the range of 20–30 μm/s.

The direction of the driving field is controlled by the orientation of the PDMS channel with respect to the array of obstacles. Therefore, we performed experiments for different angles of the driving field by changing the orientation of the channel, which was reversibly attached to the glass slide. The fact that the channel determines the direction of the driving field was verified by tracking the motion of particles inside the channel but outside the array of posts. Specifically, at the beginning of each experiment, the forcing angle relative to the obstacle array, θ, was determined experimentally by tracking the motion of particles in an obstacle-free region inside the PDMS microchannel. In order to avoid spurious correlations in the results, the experiments were not carried out in any particular decreasing or increasing order of forcing angles. The migration angle relative to the obstacle array, α, is then measured by tracking an independent set of particles moving through the array of posts. In each of the experiments, we tracked around 15–20 different particles of the same size, both in the obstacle-free region as well as inside the array. In order to reduce fluctuations in the measured migration angle, only those trajectories that are 100 μm or longer—in the horizontal direction—are considered. In addition, we only considered the motion of particles that did not interact with other particles along their trajectories. The definition of the migration and forcing angles (as well as the coordinate axes) are illustrated in Fig. 1.

The experiments were performed in the deterministic limit, that is, when the diffusive transport of the suspended particles is negligible. As an estimation, the Peclet number, calculated from the Stokes–Einstein relation for the bulk

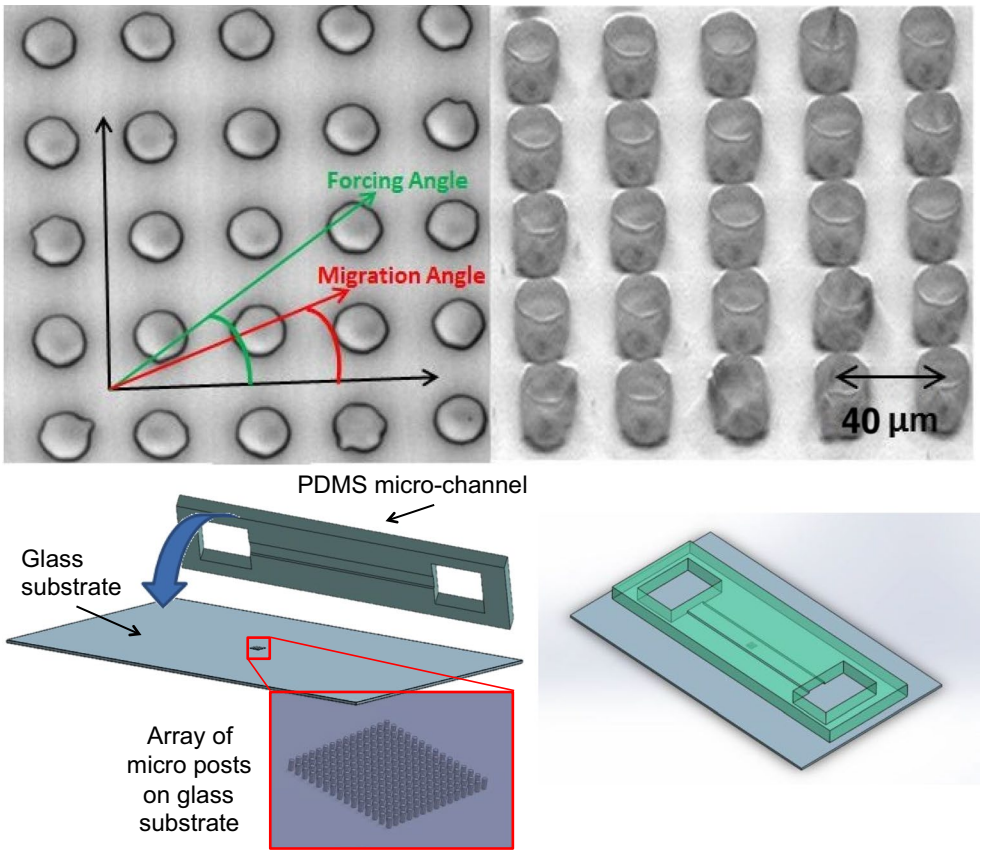

Fig. 1 (*Top*) Microscopic images of the device. (*Top-left*) *Top view*, with the definition of forcing and migration angles. (*Top-right*) *3D view* showing the height of the posts. (*Bottom*) Schematic of the experimental setup. (*Bottom-left*) Glass slide, post array, PDMS channel and reservoirs. (*Bottom-right*) Final device configuration

diffusivity of the particles and the experimentally measured average velocity, ranges from O(10^2) to O(10^4).

3 Results and discussion

We have performed a series of independent experiments to measure the migration angle of suspended particles of sizes 4.32, 10 and 15 µm electrokinetically driven through the obstacle array at forcing angles, θ, ranging from 0° to 45°, with respect to the main lattice directions (see Fig. 1). In Fig. 2, we present the migration angle, α, versus forcing angle, θ, for all particles over the complete range of forcing directions (note that each data point corresponds to independent experiments, in which the average migration angle is determined for a given forcing orientation). The vertical (horizontal) error bars represent the standard deviation in the measured migration (forcing) angles. The observed motion of the suspended particles is completely analogous to that observed in previous DLD experiments, with particles exhibiting periodic trajectories and directional locking. That is, particles move at certain lattice directions that

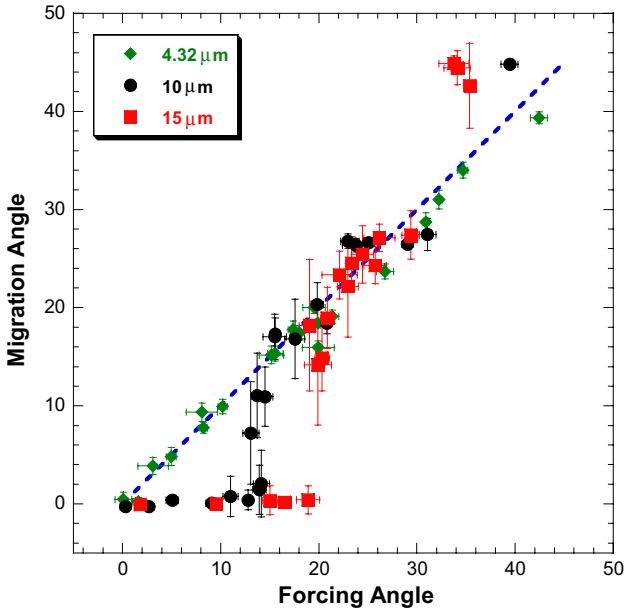

Fig. 2 Average migration angle (α) as a function of forcing angle (θ) for 4.32, 10, 15 micron particles. The *dashed diagonal line* represents $\alpha = \theta$

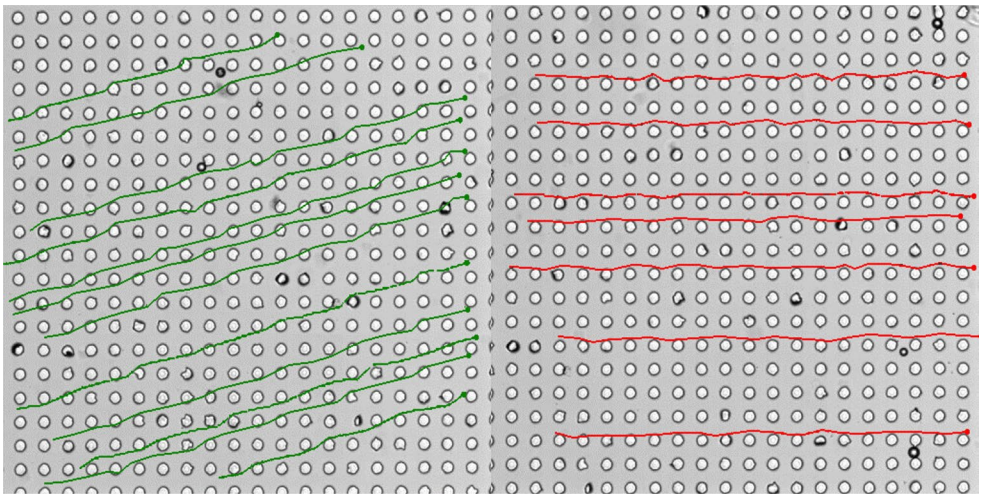

Fig. 3 Trajectories obtained for a forcing angle $\theta \sim 18°$ with (*left*) 4.32 μm and (*right*) 15 μm particles. (*left*) Smaller particles are able to closely follow the forcing angle as shown in Fig. 2. (*right*) Larger particles are locked into the [1,0] lattice direction. As a result, there is a significant difference in migration angles, nearly as large as the forcing direction

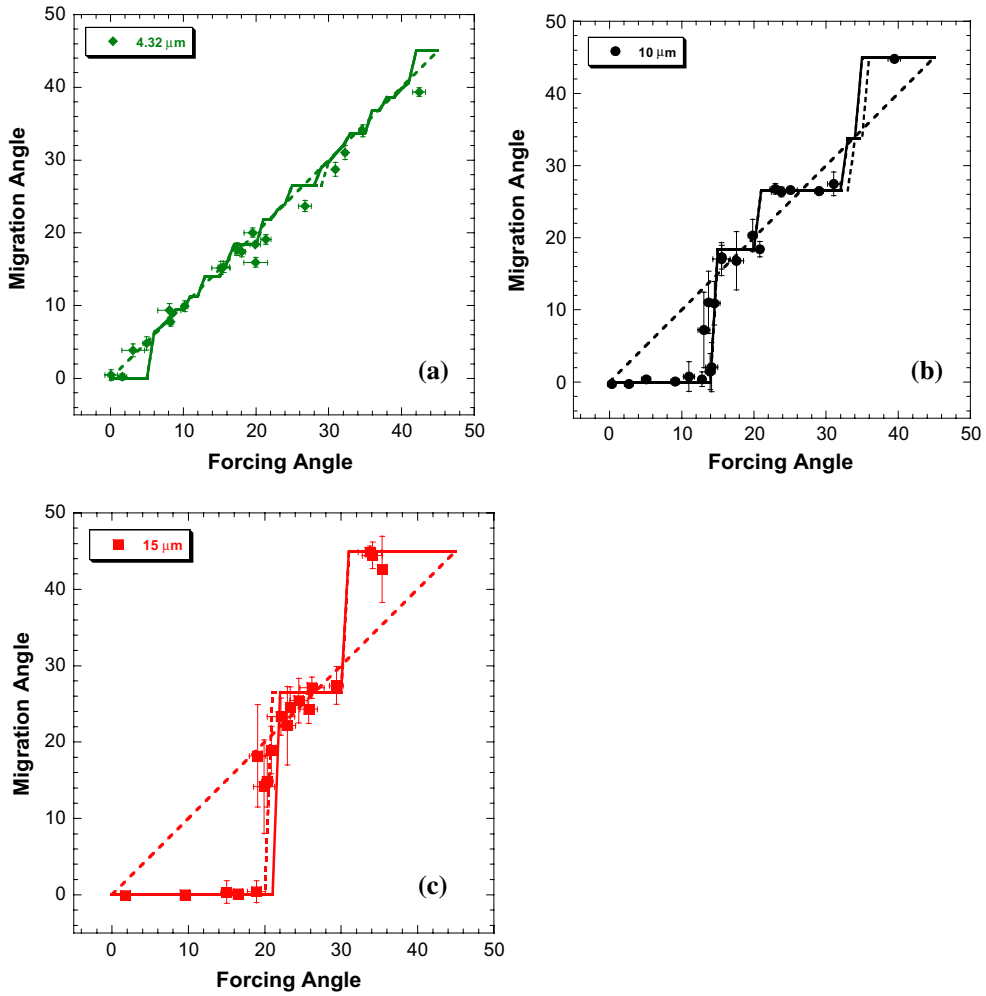

Fig. 4 Average migration angle as a function of forcing angle. The *solid lines* show the theoretical prediction with b_c as a fitting parameter. *Dashed lines* show the uncertainty in b_c. The *diagonal line* is plotted for reference and corresponds to $\alpha = \theta$. **a** 4.32 μm particles, $b_c = 2.1 \pm 0.1$; **b** 10 μm particles, $b_c = 5.2 \pm 0.1$; **c** 15 μm particles, $b_c = 7.1 \pm 0.05$

remain constant for a range of forcing angles. For example, all particles are *locked* in the [1,0] direction at small forcing angles. Essentially, particles move along a line of consecutive posts in one of the principal directions of the array (say a *column* of the array). Only at large enough forcing angles the particle move across a column of obstacles in the array and their migration angle becomes different from [1,0]. We also observe sharp transitions between locking directions, a phenomena that could be harnessed to obtain high selectivity and resolution in the separation process (Devendra and Drazer 2012). It is also clear that, at certain special forcing angles, particles of different size exhibit different migration angles, which is the basis for separation. Interestingly, the first transition angle (or *critical angle*) θ_c, defined as the largest forcing angle for which the particles are locked to move in the [1,0] direction (along a column of the array), shows the largest variation with the size of the particles, with smaller particles transitioning at smaller angles. More specifically, the smallest particles, 4.32 μm, exhibit a very early transition at $\theta \sim 5°$, while 10 μm and 15 μm particles remain locked to move in the [1,0] lattice direction until about $\theta \sim 14°$ and $\theta \sim 19°$, respectively. Therefore, a driving direction $\theta \sim 18°$ would efficiently separate the 4.32 μm particles from the 15 μm ones. In fact, in Fig. 3, we show two sets of trajectories obtained from 4.32 and 15 μm particles at $\theta \sim 18°$, and a significant difference in migration angles is evident.

Figure 4 shows the average migration angles obtained for each of the individual species. The figures also show the theoretical predictions based on a simple *collision model* developed to explain g-DLD experiments (Bowman et al. 2012; Balvin et al. 2009). In this simple model, particle–obstacle collisions might induce a net lateral displacement in the trajectory of the suspended particles, depending on the initial offset of the collision (defined as the distance between the incoming particle and the line in the direction of the driving force that goes through the center of the obstacle). Specifically, for any initial offset b smaller than a critical offset b_c, the offset after the collisions becomes equal to b_c. It is this irreversible collapse of trajectories that leads to the observed directional locking (Frechette and Drazer 2009). The value of b_c for each particle size is obtained by fitting the experimental data, is indicated in the figures, and is related to the first critical angle by $b_c = l \sin(\theta_c)$, where l is the post-to-post distance (the separation between posts in the square array). We observe that the value of the critical offset b_c increases with the size of the particles, which corresponds to the increase in the first critical angle discussed before. Overall, there is excellent agreement between the model and the experimental results for all particle sizes. Note that, b_c is the only fitting parameter, and for a given value of b_c, the model predicts all the possible locking directions as well as the forcing angles at which there is a transition in the locking directions.

4 Conclusions

We have demonstrated the basis for electrokinetically driven deterministic lateral displacement (e-DLD) for size-based separation of suspended particles in microfluidic devices. We have shown that the observed deterministic kinetics of the particles is analogous to the case of flow- and force-driven DLD, including directional locking, and our understanding of those systems can be applied to describe and analyze the behavior in the proposed e-DLD devices. We performed a comprehensive set of experiments that covered the entire range of orientations of the driving electric field, and showed the potential for separation at specific forcing angles. We also showed that the first transition angle changes significantly with particle size, with a difference of nearly 15° between the smallest and largest particles, which suggests the use of relatively small angles to optimize the resolution of the system. The differences in the critical angles, the significant difference in the migration angle between the observed locking directions (≈18° between [1,0] and [3,1] directions, or ≈26° between [1,0] and [2,1] directions), and the sharp transitions between locking directions, indicate the potential for high size resolution of the proposed e-DLD separation method.

The use of electrokinetically driven flows could significantly expand the application of DLD methods. Driving the suspension with an electric field makes the system amenable to on-line external control and reconfiguration of the forcing angle depending on the sample, something that is not straightforward in flow-driven DLD. Finally, let us mention that the use of electric fields provides ways to control or tune the operation of DLD devices, by manipulating not only particle–obstacle interactions, as shown in recent work (Beech et al. 2009) but also the spatial variations of the driving field to enhance the separative displacement among different species.

Acknowledgments This work is partially supported by the National Science Foundation Grant No. CBET-1343924. We acknowledge partial support from Office of Naval Research Award No.: N000141110019.

References

Al-Fandi M, Al-Rousan M, Jaradat MAK, Al-Ebbini L (2011) New design for the separation of microorganisms using microfluidic deterministic lateral displacement. Robot Comput Integr Manuf 27:237–244

Balvin M, Sohn E, Iracki T, Drazer G, Frechette J (2009) Directional locking and the role of irreversible interactions in deterministic

hydrodynamics separations in microfluidic devices. Phys Rev Lett 103:078301
Beech JP, Tegenfeldt JO (2008) Tuneable separation in elastomeric microfluidics devices. Lab Chip 8:657–659
Beech JP, Jonsson P, Tegenfeldt JO (2009) Tipping the balance of deterministic lateral displacement devices using dielectrophoresis. Lab Chip 9:2698–2706
Bowman T, Frechette J, Drazer G (2012) Force driven separation of drops by deterministic lateral displacement. Lab Chip 12: 2903
Bowman TJ, Drazer G, Frechette J (2013) Inertia and scaling in deterministic lateral displacement. Biomicrofluidics 7:064111
Chang S, Cho Y-H (2008) A continuous size-dependent particle separator using a negative dielectrophoretic virtual pillar array. Lab Chip 8:1930–1936
Cummings EB (2003) Streaming dielectrophoresis for continuous-flow microfluidic devices. IEEE Eng Med Biol Mag 22:75–84
Cummings EB, Singh AK (2003) Dielectrophoresis in microchips containing arrays of insulating posts: theoretical and experimental results. Anal Chem 75:4724–4731
Davis JA et al (2006) Deterministic hydrodynamics: taking blood apart. Proc Natl Acad Sci 103:14779–14784
Devendra R, Drazer G (2012) Gravity driven deterministic lateral displacement for particle separation in microfluidic devices. Anal Chem 84:10621–10627
Devendra R, Drazer G (2014) Deterministic fractionation of binary suspensions moving past a line of microposts. Microfluid Nanofluidics 17:519–526
Frechette J, Drazer G (2009) Directional locking and deterministic separation in periodic arrays. J Fluid Mech 627:379–401
Green JV, Radisic M, Murthy SK (2009) Deterministic lateral displacement as a means to enrich large cells for tissue engineering. Anal Chem 81:9178–9182
Herrmann J, Karweit M, Drazer G (2009) Separation of suspended particles in microfluidic systems by directional locking in periodic fields. Phys Rev E 79:061404
Holm SH, Beech JP, Barrett MP, Tegenfeldt JO (2011) Separation of parasites from human blood using deterministic lateral displacement. Lab Chip 11:1326–1332
Huang LR, Cox EC, Austin RH, Sturm JC (2004) Continuous particle separation through deterministic lateral displacement. Science 304:987–990
Huang R et al (2008) A microfluidics approach for the isolation of nucleated red blood cells (NRBCs) from the peripheral blood of pregnant women. Prenat Diagn 28:892–899
Hunter RJ (1981) Zeta potential in colloid science: principles and applications. Academic Press, New York
Inglis DW, Davis JA, Austin RH, Sturm JC (2006) Critical particle size for fractionation by deterministic lateral displacement. Lab Chip 6:655–658
Inglis DW, Lord M, Nordon RE (2011) Scaling deterministic lateral displacement arrays for high throughput and dilution-free enrichment of leukocytes. J Micromech Microeng 21:054024
Joensson HN, Uhlén M, Svahn HA (2011) Droplet size based separation by deterministic lateral displacement—separating droplets by cell-induced shrinking. Lab Chip 11:1305–1310
Li N, Kamei DT, Ho C-M (2007) On-chip continuous blood cell subtype separation by deterministic lateral displacement. In: 2nd IEEE International Conference on Nano/Micro Engineered and Molecular Systems, 2007. NEMS'07 (IEEE), pp 932–936. doi:10.1109/NEMS.2007.352171
Loutherback K et al (2010) Improved performance of deterministic lateral displacement arrays with triangular posts. Microfluid Nanofluidics 9:1143–1149
Masliyah JH, Bhattacharjee S (2006) Electrokinetic and colloid transport phenomena. Wiley, Hoboken
Morton KJ et al (2008a) Crossing microfluidic streamlines to lyse, label and wash cells. Lab Chip 8:1448–1453
Morton K et al (2008b) Hydrodynamic metamaterials: microfabricated arrays to steer, refract, and focus streams of biomaterials. Proc Natl Acad Sci USA 105:7434–7438
Pamme N (2007) Continuous flow separations in microfluidic devices. Lab Chip 7:1644–1659
Paul PH, Garguilo MG, Rakestraw DJ (1998) Imaging of pressure- and electrokinetically driven flows through open capillaries. Anal Chem 70:2459–2467
Risbud SR, Drazer G (2013) Trajectory and distribution of suspended non-Brownian particles moving past a fixed spherical or cylindrical obstacle. J Fluid Mech 714:213–237
Sureda M, Miller A, Diez FJ (2012) In situ particle zeta potential evaluation in electroosmotic flows from time-resolved microPIV measurements. Electrophoresis 33:2759–2768
Xuan J, Lee ML (2013) Size separation of biomolecules and bioparticles using micro/nanofabricated structures. Anal Methods 6:27–37
Yan D, Yang C, Nguyen N-T, Huang X (2006) Electrokinetic flow in microchannels with finite reservoir size effects. J Phys Conf Ser 34:385–392
Zeming KK, Ranjan S, Zhang Y (2013) Rotational separation of non-spherical bioparticles using I-shaped pillar arrays in a microfluidic device. Nat Commun 4:1625
Zhang B, Green JV, Murthy SK, Radisic M (2012) Label-free enrichment of functional cardiomyocytes using microfluidic deterministic lateral flow displacement. PLoS One 7:e37619